Accepted Manuscript

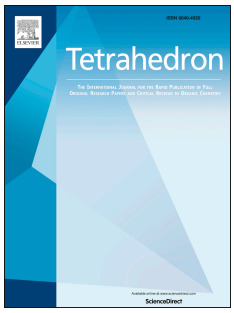

A bio-inspired cascade and a late-stage directed sp^3 C-H lithiation enables a concise total synthesis of (−)-virosaine A

Jonathan M.E. Hughes, James L. Gleason

PII: S0040-4020(17)31286-3

DOI: 10.1016/j.tet.2017.12.026

Reference: TET 29182

To appear in: *Tetrahedron*

Received Date: 5 September 2017

Revised Date: 7 December 2017

Accepted Date: 12 December 2017

Please cite this article as: Hughes JME, Gleason JL, A bio-inspired cascade and a late-stage directed sp^3 C-H lithiation enables a concise total synthesis of (−)-virosaine A, *Tetrahedron* (2018), doi: 10.1016/j.tet.2017.12.026.

Graphical Abstract

To create your abstract, type over the instructions in the template box below.
Fonts or abstract dimensions should not be changed or altered.

A bio-inspired cascade and a late-stage directed sp^3 C-H lithiation enables a concise total synthesis of (-)-virosaine A

Leave this area blank for abstract info.

Jonathan M. E. Hughes and James L. Gleason*
Department of Chemistry, McGill University, 801 Sherbrooke St. West, Montréal, Québec, H3A 0B8, Canada

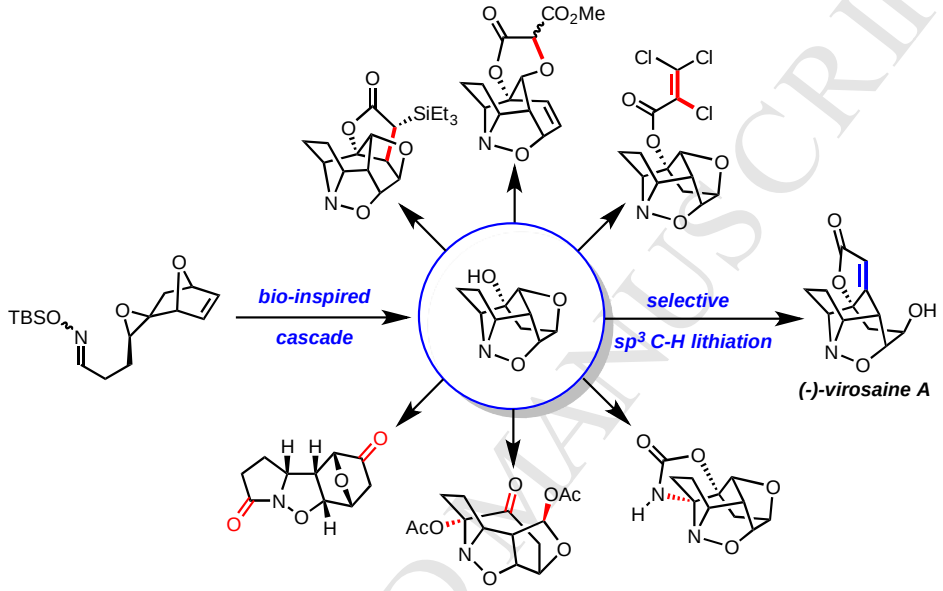

Tetrahedron
journal homepage: www.elsevier.com

A bio-inspired cascade and a late-stage directed sp^3 C-H lithiation enables a concise total synthesis of (-)-virosaine A

Jonathan M. E. Hughes, James L. Gleason*

Department of Chemistry, McGill University, 801 Sherbrooke St. West, Montréal, Québec, H3A 0B8 Canada

ARTICLE INFO

Article history:
Received
Received in revised form
Accepted
Available online

Keywords:
Alkaloids
Cascade reactions
Total synthesis
Directed lithiation
Cycloaddition

ABSTRACT

The asymmetric total synthesis of (-)-virosaine A was achieved in 9% overall yield from commercially/readily available starting materials. Inspired by an intriguing biosynthetic proposal, a novel cascade reaction sequence was developed to efficiently construct the caged polycyclic core of virosaine A. The pivotal cascade precursor was readily available in enantiopure form *via* a robust route that featured an enantioselective one-pot Diels-Alder cycloaddition/organolithium addition. Several contemporary methods of C-H functionalization were applied to the cascade product and yielded a diverse set of novel complex polycycles. Ultimately, a combination of NMR and computational analyses laid the groundwork for a successful directed lithiation strategy to selectively functionalize the caged core and complete the total synthesis of virosaine A.

1. Introduction

The *Securinega* alkaloids are a fascinating class of secondary plant metabolites found within the Euphorbiaceae family.[1] The structural characteristics of these natural products, typified by their bridged tetracyclic scaffolds and an intriguing α,β,γ,δ-unsaturated lactone moiety, have provided a continual source of inspiration for synthetic chemists.[2] Securinine (**1**), the parent member of this family, was isolated more than 60 years ago and has been the most extensively studied *Securinega* alkaloid (Figure 1). It exhibits an extensive biological activity profile and was for a time marketed as a drug for its stimulant and antiplasmodic effects.[1] Its intriguing profile and structure spurred numerous synthetic efforts which have culminated in a number of elegent total syntheses.[3] As isolation efforts of this natural product class progressed, several highly oxidized and/or rearranged members emerged. Virosaine A (**3**) and B (**4**), isolated in 2012 from the twigs and leaves of *Flueggea virosa* in China, are two such examples that have undergone additional skeletal oxidation and reorganization to yield unprecedented caged polycycles.[4] The virosaines (**3** and **4**) are arguably the most complex monomeric members of this alkaloid family and, interestingly, are pseudoenantiomers, inverted at all stereocenters except C8.[5] They contain several notable structural features that make them particularly challenging synthetic targets. These include the presence of multiple bridged bicycles, six congested stereocenters and, perhaps most intriguingly, an isoxazolidine ring embedded in the pentacyclic framework. The latter is particularly noteworthy, as it is an extremely rare structural motif in natural products and has intriguing biosynthetic origins (*vide infra*).[6] Interestingly, an isoxazolidine moiety is also present in the related *Securinega* alkaloid flueggine A (**5**), uniting the two monomeric fragments from which this dimer is constructed.[7]

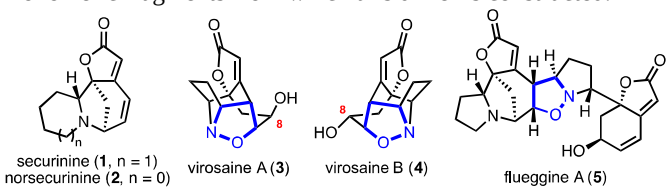

Figure 1. *Securinega* alkaloids.

The biosynthetic proposals for the virosaines (**3** and **4**) and flueggine A (**5**) all involve a union of cyclic imine **6** with arylpyruvic acid **7** to produce one of three diastereomeric tricyclic intermediates **8a**, **8b**, or **8c** (Scheme 1).[4,7,8] Direct oxidation of **8a** and **8b** is suggested to generate nitrones **9** and **10**, respectively, which are proposed to undergo subsequent intramolecular [3+2] cycloaddition to produce virosaine A (**3**) and B (**4**). Of note, synthetic studies suggest that the biosyntheses of **3** and **4** may involve the intermediacy of other *Securinega* alkaloids. Gademann demonstrated that the bubbialidine core could be oxidized/rearranged to access nitrone **9** and Yang and Li showed that nitrone **10** could be accessed from allonorsecurinine in a similar fashion.[9] In the case of flueggine A (**5**), intramolecular dehydration of **8c** generates norsecurinine (**2**), which is then proposed to undergo oxidation/rearrangement to generate nitrone **12**. However, **12**

* Corresponding author. Tel.: +1-514-398-5596; fax: +1-514-398-3797; e-mail: jim.gleason@mcgill.ca

interestingly does not undergo an intramolecular [3+2] nitrone cycloaddition, presumably due to increased non-bonding interactions incurred in the alternative caged framework that would be formed with this diastereomer.[10] Instead, **12** reacts with norsecurinine (**2**) in an intermolecular sense to produce the dimer flueggine A (**5**). Evidence to support the feasibility of these rare biosynthetic nitrone cycloadditions have mounted in recent years *via* both biomimetic syntheses and computational studies, the latter of which suggest that the energy barriers required for these cycloadditions are low enough such that enzymatic intervention is not required.[11,12,13]

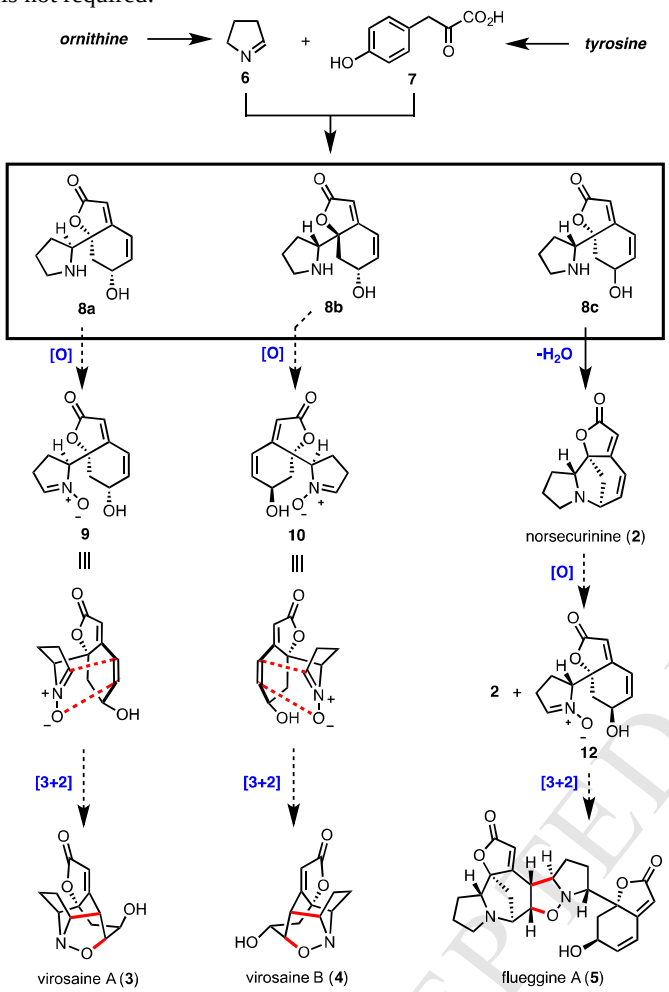

Scheme 1. Proposed biosyntheses of the virosaines (**3** and **4**) and flueggine A (**5**).

The synthetically challenging characteristics and unique biosynthetic origin of **3** motivated us to pursue its total synthesis. In particular, at the time we began our studies, the putative [3+2] dipolar cycloaddition had not been investigated synthetically. We thus embarked on a bio-inspired approach that would feature the nitrone cycloaddition as an integral step. However, in contrast to the subsequently reported syntheses that generated the nitrone via oxidative cleavage of a tertiary amine, our route employed an epoxide opening to generate the nitrone followed in tandem by the dipolar cycloaddition. Moreover, the route was enabled by the selective late-stage manipulation of an unactivated C(sp^3)-H bond in a pentacyclic intermediate, resulting in a short, efficient synthesis. Herein, the evolution and full details of these efforts are reported.[14]

2. Synthetic Plan

2.1 Retrosynthetic analysis.

Retrosynthetically, we identified lactone **13** as precursor of **3** that effectively masks both the butenolide and C8 hydroxyl groups (Scheme 2). Hexacycle **13** could be simplified to pentacycle **14**, with an unspecified R group at C14 that could eventually be elaborated into the butanolide in **13**. Drawing inspiration from the proposed biosynthesis, we traced pentacycle **14** back to the corresponding nitrone **15** *via* a [3+2] nitrone cycloaddition. In order to install the requisite nitrone, we planned to open a trisubstituted epoxide with a pendant oxime, leading back to **16**. The advantage of this method is that it would build the nitrone in a stereospecific fashion and would eliminate any concerns of chemo- or regioselectivity compared to oxidative methods of nitrone formation. Furthermore, our goal was to implement this epoxide-opening step in tandem with the subsequent nitrone cycloaddition (**16**→**15**→**14**). The development of such a cascade reaction sequence would enable an efficient entry into the complex polycyclic virosaine core. Finally, we traced the cascade precursor **16** back to aldehyde **17**, the [4+2] cycloadduct of 2-bromoacrolein (**18**) and substituted furan **19**.[15]

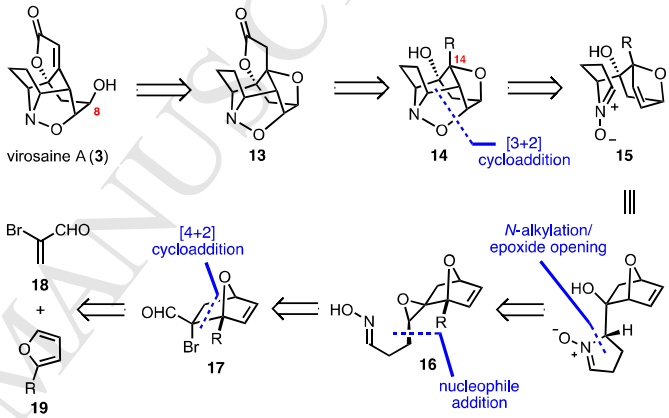

Scheme 2. Original retrosynthetic analysis of **1**.

3. Results and Discussion

3.1 Model cascade reaction sequence.

Given that the proposed bio-inspired cascade reaction sequence to access the caged pentacycle **14** was a focal point of the synthetic plan, we initially pursued a model study to assess the feasibility of this approach. Cascade reactions involving tandem nitrone formation/[3+2] cycloaddition have provided a platform for rapid complexity generation in several total syntheses.[16] However, there is limited literature precedent for cascades that specifically involve an intramolecular epoxide opening/intramolecular nitrone cycloaddition, with only one reported example prior to our work. Specifically, Grigg and coworkers demonstrated that heating an acyclic substrate containing an oxime, epoxide, and olefin resulted in *N*-alkylative epoxide opening to generate a nitrone that underwent a subsequenct [3+2] cycloaddition to yield an angularly fused tricycle.[17] To the best of our knowledge, there were no examples of such a cascade to access bridged systems similar to that found in the virosaine core.

We identified acyclic epoxy oxime **20** as a simplified model substrate for our proposed cascade transformation (Scheme 3). The synthesis of oxime **20** commenced with sequential silyl protection and allylation of alkynol **23** to provide enyne **24** in excellent yield over two steps (Scheme 4). Stereoselective reduction of **24** to the corresponding *cis* skipped diene was achieved using nickel boride/H_2.[18,19,20] Subsequent chemoselective oxidation of the internal olefin was achieved using *m*-CPBA to yield epoxide **25** in 52% yield over two steps.

Protecting group removal and oxidation to aldehyde **26** proceeded without incident and then oxime **20** was prepared through condensation of **26** with NH_2OH.

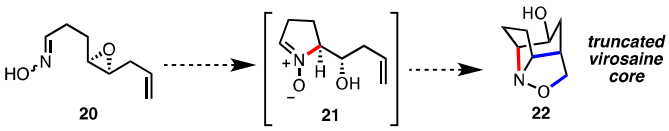

Scheme 3. Proposed cascade reaction sequence to access a truncated virosaine core **22**.

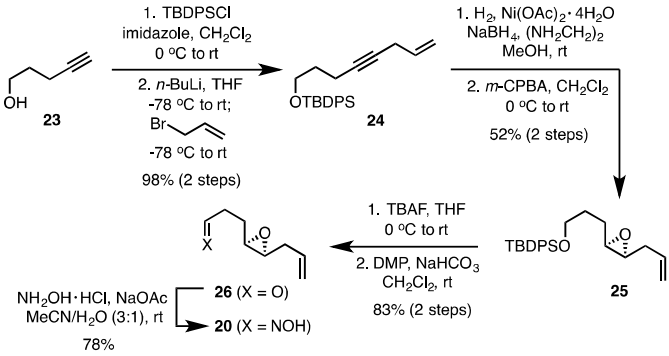

Scheme 4. Synthesis of model cascade precursor **20**.

With the model oxime **20** in hand, we investigated the epoxide-opening/nitrone cycloaddition cascade reaction sequence to access the bridged tricycle **22** (Scheme 5). Following the report by Grigg and coworkers, we initially heated **20** in xylenes at 140 °C and were pleased to find that the desired product **22** was generated. However, the yield of the overall process suffered due to the sluggish nature of the initial epoxide-opening step. As a result, extended reaction times were required to drive the reaction to completion and led to significant decomposition. This observation led us to the use of additives to promote the epoxide opening step. Ultimately we found that the use of protic acids, such as *para*-toluenesulfonic acid (*p*-TSA), promoted *N*-alkylation at room temperature to generate nitrone **21** in 81% yield. Gratifyingly, heating **21** in xylenes effected the [3+2] cycloaddition to produce **22** in 78% yield as a 7:1 mixture alongside the regioisomeric cycloadduct **27**. Furthermore, we were pleased to find that the use of catalytic protic acid at elevated temperatures (5 mol % PPTS, xylenes, 140 °C) generated **22** in 48% yield in a single pot process from oxime **20**, thereby establishing the feasibility of this cascade approach to access a simplified bridged virosaine core. Interestingly, during these studies, we found that significantly different outcomes resulted depending upon the additive employed. For example, adding LiCl produced oxazine **28** as the major product, *via* *O*-alkylation of the oxime to open the epoxide. In contrast, using K_2CO_3 generated nitrile **29** in 65% yield, presumably via initial *O*-alkylation to give oxazine **28** followed by subsequent base-mediated Kemp elimination.[21] Evidence to support this proposal was gained by subjecting **28** to the same reaction conditions, which resulted in clean conversion to nitrile **29** in 84% yield.

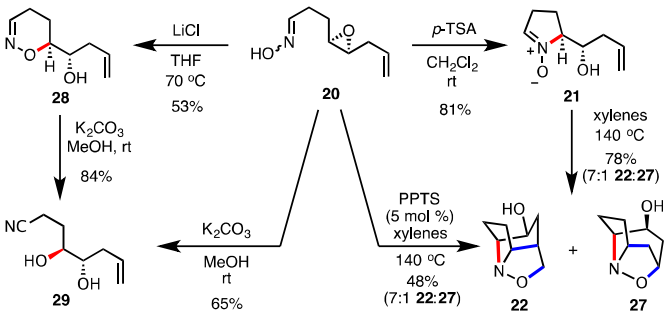

Scheme 5. Cascade reaction sequence of model oxime **20** to access the truncated virosaine core **22**.

*3.2 Attempted Diels-Alder reaction of 2-bromoacrolein (**18**) and ethyl 2-(furan-2-yl)acetate (**19**, R = CH_2CO_2Et).*

With the feasibility of the bio-inspired cascade reaction sequence established, we turned our attention to the Diels-Alder reaction required to construct oxabicyclo[2.2.1]heptene **17**.[22] The enantioselective Diels-Alder reaction of furan (**19**, R = H) with 2-bromoacrolein (**18**) was previously reported by Corey and appeared well suited to our needs.[23] To this end, we attempted the cycloaddition of ethyl 2-(furan-2-yl)acetate (**19**, R = CH_2CO_2Et) with 2-bromoacrolein (**18**) by allowing them to react in the presence of oxazaborolidinone catalyst **30** (Scheme 6). However, to our dismay, the only products generated in the reaction were furans **31** and **32**, resulting from a Friedel-Crafts conjugate addition. Disappointingly, modifying the reaction conditions (reaction time, temperature, catalyst, quenching method, *etc.*) did not alter the course of the reaction and either generated **31** and **32**, in varying amounts, or resulted in polymerization of **18**.[24] Several other substituted furans (**19**, R = OMe, Me, TMS) yielded similarly disappointing results.

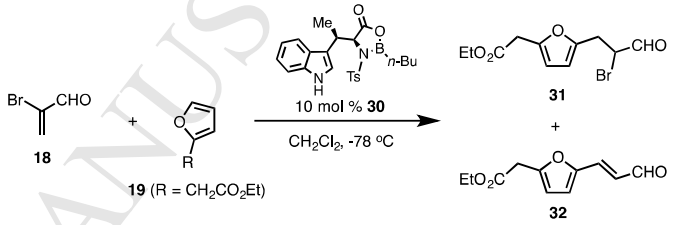

Scheme 6. Reaction of 2-bromoacrolein (**18**) with ethyl 2-(furan-2-yl)acetate (**19**, R = CH_2CO_2Et).

This limitation of the furan Diels-Alder reaction presented a significant problem as our proposed route relied on the [4+2] cycloaddition to install requisite functionality in **14** to ultimately generate the butenolide in **3** (*vide supra*). Faced with this unanticipated obstacle, we considered the use of known oxabicycle **33**, resulting from cycloaddition with furan rather than its substituted congeners, within our proposed route to access pentacycle **34** (Scheme 7).[23] However, this subtle change had a significant consequence in that it would require the implementation of a selective late-stage functionalization at C14 of **34** to construct butanolide **13**. While late-stage C-H functionalization strategies have proven enabling in total synthesis, their successful implementation can be challenging within complex molecular frameworks.[25,26] In this particular case, the presence of the isoxazolidine and 12 distinct C-H bonds make selective functionalization of **34** an ambitious task. Nevertheless, we were greatly motivated to pursue this strategy as it not only would enable our proposed cascade reaction sequence but also, together, these key transformations would allow us to prepare **3** in a highly efficient manner.

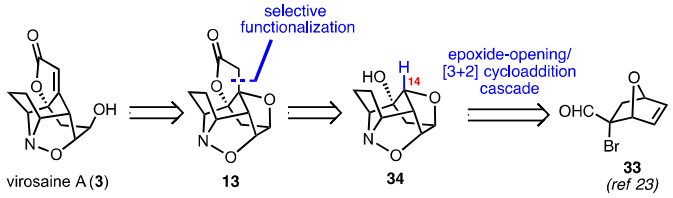

Scheme 7. Late-stage C14 functionalization strategy to access **3** *via* oxabicycle **33**.

*3.3 Synthesis of cascade precursor **44**.*

We prepared Corey's oxabicycle **33** by combining 2-bromoacrolein (**18**) with furan (**35**) in the presence of oxazaborolidinone **30** at –78 °C in CH_2Cl_2 (Scheme 8).[23] In our hands, **33** was difficult to isolate in high yield or purity and readily underwent cycloreversion to return starting materials. Similar observations with bicycle **33** were made by Carreira, who opted to trap the aldehyde *in situ* by addition of either an enolate, silyl ketene acetal, or $NaBH_4$.[27] We examined a similar approach to trap **33** *in situ* with a Grignard or equivalent nucleophile to access a bromohydrin product that was expected to be more stable. Initially, we found that allyl and 3-butenylmagnesium bromide could be added to the unstable aldehyde to provide bromohydrins **36** and **37**, respectively. In both cases, the products were generated with negligible diastereoselectivity. Moreover, the terminal olefins in **36** and **37** could not be selectively manipulated in the presence of the strained internal olefin and prompted us to examine other nucleophiles. Ultimately, thorough screening led us to identify organolithium **38** as the most selective nucleophile, providing the desired bromohydrin product **39** in 62% yield and in a favorable, albeit modest, 2.7:1 d.r. and 83% *ee*.[28] Interestingly, in studying this reaction, we found that the yield and *ee* of bromohydrin **39** was highly dependent on the method used to generate the oxazaborolidinone Diels-Alder catalyst **30**. Specifically, we found that the best yield and *ee* values were obtained when **30** was generated using neat *n*-butyldichloroborane,[27c] while using either *n*-butylboronic acid or a toluene solution of *n*-butyldichloroborane provided inferior results. Furthermore, while the two bromohydrin diastereomers were inseparable by chromatography, we were gratified to find that recrystallization delivered the desired diastereomer **39** in >20:1 d.r. and >99% *ee*. Overall, this one-pot process efficiently installed 10 of the 12 carbon atoms and 3 of the 6 stereocenters of the natural product.

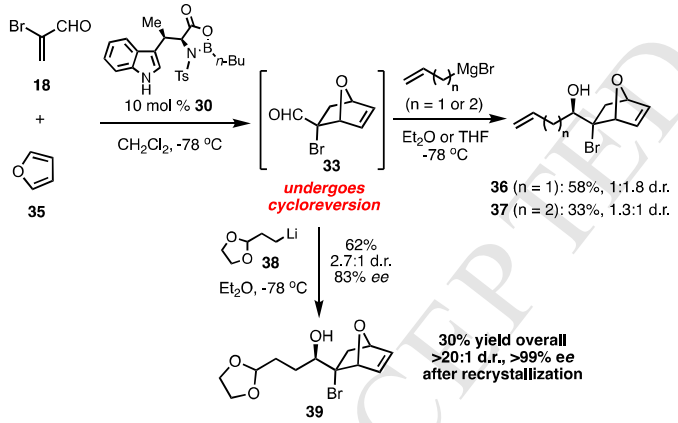

Scheme 8. Enantioselective synthesis of bromohydrin **39**.

With an efficient process established for the generation of **39**, we focused on its elaboration to the key cascade precursor. Initially, we found that bromohydrin **39** could be cleanly converted to the corresponding epoxide **40** by treatment with K_2CO_3 in MeOH (Scheme 9). The stereochemical assignment of **39** was unambiguously confirmed by an observed nuclear Overhauser effect (nOe) between the epoxide proton and the axial proton of the bridged bicycle in **40**. Unfortunately, attempted acid-mediated dioxolane removal failed to reveal the latent aldehyde **41** and led to decomposition of material and/or complex mixtures in every case. Alternatively, we found that the dioxolane protecting group could be removed directly from bromohydrin **39** under mildly acidic conditions to provide the corresponding lactol **42** in near quantitative yield. All attempts at base-mediated conversion of **42** to aldehyde **41** were met with failure. However, we found that lactol **42** could be directly converted to *O*-silylated oxime **43** by treatment with $TBSONH_2$ in the presence of molecular sieves. Finally, treatment of **43** with NaH effected smooth conversion to epoxide **44**, a protected analogue of our cascade precursor. Importantly, we found that the silyl protecting group was critical to the success of this epoxide formation. In contrast, the corresponding unprotected oxime failed to undergo bromide displacement and, instead, produced cyclic aminal **45,** which could not be converted to epoxide **16**.

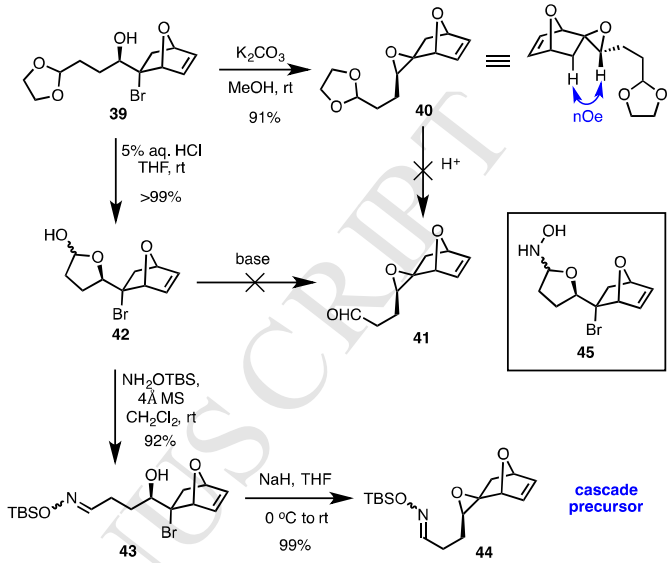

Scheme 9. Synthesis of cascade precursor **44**.

*3.4 Cascade reaction sequence optimization to access the virosaine core **34**.*

The development of a robust route to access the oxime epoxide set the stage for the study of the key cascade reaction sequence to prepare the pentacyclic virosaine core **34** (Table 1). Initial cascade studies were conducted on the free oxime **16** (R = H, see Supporting Information for preparation) and, gratifyingly, submission to the reaction conditions that were developed during the initial model studies afforded **34** as the sole product in a promising 26% yield (entry 1).[29] Encouraged by these results, we examined direct cascade reactions using silyl oxime **44**. The amount of PPTS was increased to 1 equivalent in order to facilitate silyl group cleavage and we examined more polar solvents due to the low solubility of PPTS in xylenes. We found that the cyclization occurred in both THF and MeCN with significantly improved yields (entries 3 and 4), while MeOH did not lead to any significant improvement (entry 5). Additionally, we found that using microwave heating in place of conventional heating led to a significant decrease in reaction time (entry 2 vs. 3). Among the additives assessed, both BF_3•OEt_2 and HF were found to be detrimental to reaction, producing only trace amounts of **34**, at best (entries 6 and 7). Importantly, while acetic acid was not an efficient promoter when employed as an additive in acetonitrile (entry 8), the reaction conducted in acetic acid as solvent afforded **34** in 78% yield (entry 9). Furthermore, we were pleased to find that by reducing the reaction time to 30 minutes, **34** could be isolated in an excellent 92% yield (entry 10). Moreover, the reaction could also be conducted on gram scale (5.2 mmol) using conventional heating, to produce the virosaine core in only a slightly diminished 82% yield (entry 11). Overall, this novel cascade process allowed us to access the complex core of virosaine A (**3**) in only 5 steps from commercially available materials.

Table 1. Cascade reaction sequence optimization.

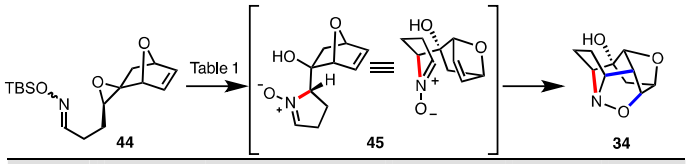

Entry	Solvent	Acid (equiv.)	Temp (°C)	Time	Yield (%)[a]
1[b]	xylenes	PPTS (0.2)	140	8 h	26
2	THF	PPTS (1)	70	12 h	40
3[c]	THF	PPTS (1)	100	1 h	45
4[c]	MeCN	PPTS (1)	120	1 h	50
5[c]	MeOH	PPTS (1)	120	1 h	28
6	CH_2Cl_2	BF_3•OEt_2 (2)	0 → 45	17 h	0
7	MeCN	HF in H_2O (5)	22 → 70	15 h	trace
8[c]	MeCN	AcOH (5)	120	1 h	<10[d]
9[c]	AcOH	-	120	1 h	78
10[c]	AcOH	-	120	30 min	92
11[e]	AcOH	-	120	40 min	82

[a]Isolated yields of **34**. [b]Oxime **16** (R = H) used as starting material. [c]Microwave heating. [d]Recovered 89% starting material. [e]5.2 mmol scale.

3.5 Carbene C-H insertion strategies to functionalize C14 of the virosaine core.

With an efficient route in place to access the polycyclic virosaine core, the final obstacle was selective C14 functionalization to install the butanolide ring. Direct selective functionalization of **34** would likely be a challenging task due to potential difficulties associated with controlling regioselectivity in the presence of 12 distinct C-H bonds and chemoselectivity in the presence of the basic isoxazolidine. However, the presence of the C10 hydroxy as a tethering point opened the possibility to carry out an intramolecular functionalization, effectively limiting the potential sites of reactivity to the C2 methine, the C9 methylene and the (desired) C14 methine (Figure 2).

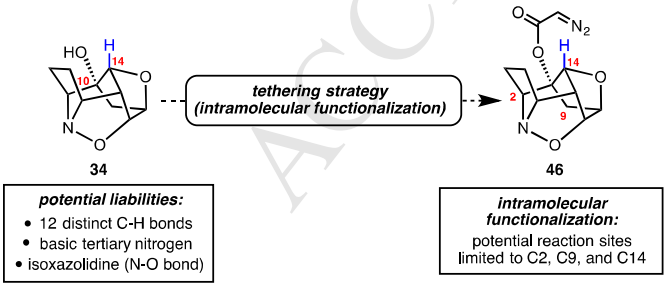

Figure 2. Tethering strategy for intramolecular functionalization of the virosaine core.

The most direct route to access **3** via a C-H modification was through an intramolecular C-H insertion reaction of diazoacetate **46** to prepare lactone **13**.[30] There are only a few successful examples of carbene C-H insertions at bridgehead positions reported in the literature and challenges associated with their implementation have been noted in several cases.[31] Nevertheless, the potential directness of this route merited investigation. Accordingly, diazoacetate **46** was prepared from **34** in a high-yielding one-pot procedure involving sequential diketene addition, diazo transfer, and deacetylation (Scheme 10). With **46** in hand, we surveyed several common Rh^{2+} and Cu^{2+} catalysts but were disappointed to find that complex, inseparable mixtures of products were generated in every case. As a result, we turned our attention to the corresponding silyl diazoacetate **47**, which was prepared by treating **46** with Et_3SiOTf. Silyl diazoacetates have previously been shown to attenuate C-H insertion reactivity and, consistent with this observation, metal-catalyzed reactions of **47** resulted in fewer undesired byproducts than reactions of the parent diazoacetate **46**.[31d] Moreover, several Rh^{2+} catalysts produced a single C-H insertion product, with $Rh_2(NHC(O)CF_3)_4$ providing the highest isolated yield. Unfortunately, structural analysis revealed this product to be silyllactone **48**, resulting from C-H insertion into the C9 methylene. Interestingly, in addition to the lactone product **48**, butyrate **49** was consistently generated in minor amounts, presumably *via* a silyl carbene rearrangement.[32]

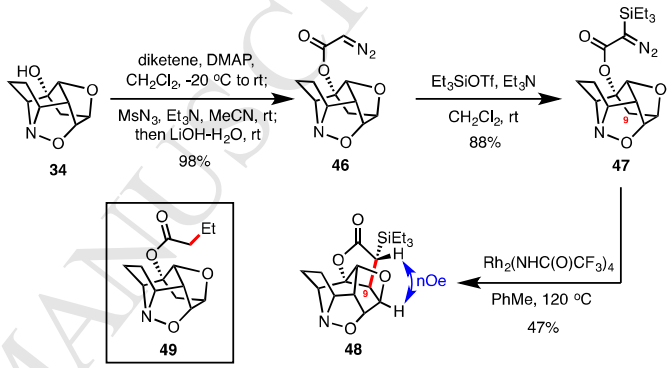

Scheme 10. Carbene insertion of silyl diazoacetate **47**.

To study the consequence of modifying the substrate electronics on the carbene insertion process, we prepared diazomalonate **51** by acylation of **34** with methyl malonyl chloride followed by diazo transfer on the intermediate malonate **50** (Scheme 11). Intriguingly, when diazomalonate **51** was treated with catalytic amounts of either $Rh_2(OAc)_4$ or $Rh_2(NHC(O)CF_3)_4$, the major product was ether **53**. The mechanism for the formation of **53** likely involves trapping of the highly electrophilic rhodium carbenoid by an oxygen lone pair to generate oxonium ylide **52**. An elimination/protonation process would then deliver the observed product **53**.[33]

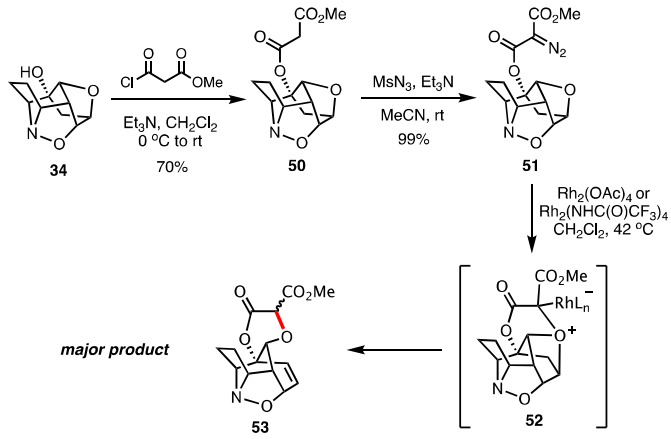

Scheme 11. Reactions of diazomalonate **51** to form cyclic ether **53**.

We considered whether the undesired reactivity observed in the attempted metal-catalyzed carbene insertions might be due to the sterics associated with the large rhodium carbenoid. This prompted us to explore the possibility of using a free carbene to

insert into the C14-H14 bond. Accordingly, solutions of diazoacetates **46** and **47** in CCl_4 were exposed to ultraviolet light (254 nm). However, under these conditions, the only products generated in the reaction were perchlorinated esters **54** and **55** resulting from exclusive reaction with the solvent itself. Changing the reaction medium to the less reactive $PhCF_3$ did not prove beneficial and, in the case of both diazoacetate substrates, complex mixtures of products were generated. In the case of silyl diazoacetate **47**, several products could be assigned from the crude reaction mixture. These included three previously known compounds (alcohol **34**, silyllactone **48**, and butyrate **49**) as well as oxygen trapping / elimination product **56** (tentative assignment). These results indicated that a free carbene was far from selective and was unlikely to deliver the desired C-H insertion product in high yield, if at all.

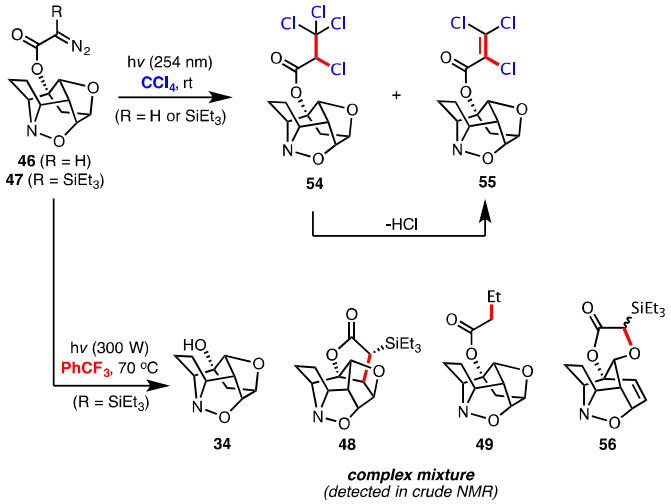

Scheme 12. Photolytic carbene generation from diazoacetates **46** and **47**.

As a final attempt at using a carbene C-H insertion to functionalize C14, we attempted an intermolecular carbene insertion. Specifically, we exposed the TMS-protected virosaine core **57** to ethyl diazoacetate in the presence of catalytic $Rh_2(OAc)_4$ (Scheme 13). However, the only product generated in the reaction was aminal **58** resulting from a formal N-O carbene insertion. Perhaps unsurprisingly, the formation of **58** likely occurs *via* trapping of a rhodium carbenoid intermediate by the isoxazolidine nitrogen of **57**. This would lead to aza ylide **59**, which can undergo subsequent Stevens rearrangement. While this result was clearly undesired, to the best of our knowledge, this is the first example of a carbene insertion into an isoxazolidine N-O bond.[34] In addition, this transformation clearly highlights the difficulties of employing an intermolecular functionalization strategy in the presence of the reactive isoxazolidine unit.

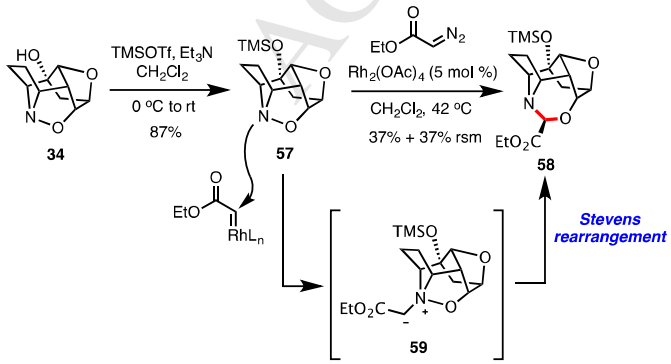

Scheme 13. Intermolecular carbene N-O insertion.

3.6 Nitrene C-H insertion strategy to functionalize C14 of the virosaine core.

The inability of the carbenes to insert into the bridgehead position can potentially be attributed to several factors, such as the steric environment around C14 and/or the silyl rhodium carbenoid as well as the presence of other reactive functional groups in the system. As an alternative to this approach, we considered the corresponding nitrene C-H insertion reactions, which have seen considerable development throughout the past two decades and have enjoyed widespread utility in the synthesis of natural products.[35,36] Furthermore, there are several reports of the use of intramolecular nitrene C-H insertions to functionalize bridgehead positions in complex molecular settings.[26a,26f,36e-g] Although a nitrene insertion at C14 in a carbamate such as **60** would not introduce the butanolide directly, hydrolysis of the resulting oxazolidinone would reveal a ketone (e.g. **62**) which might be amenable to further manipulation to ultimately produce **3** (Scheme 14).

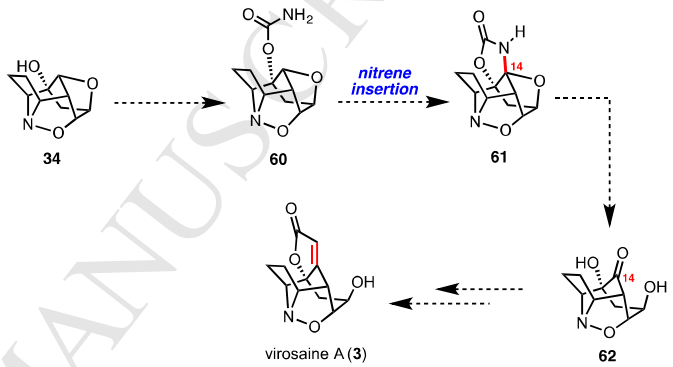

Scheme 14. Proposed nitrene C-H insertion route to functionalize C14 and access virosaine A (**3**).

Carbamate **60** was prepared in near quantitative yield from alcohol **34** through sequential reaction with $Cl_3CC(O)NCO$ and $NaHCO_3$/MeOH (Scheme 15). With **60** in hand, we screened various nitrene generating conditions and quickly identified He's conditions [$PhI(OAc)_2$, AgOTf, bathophenanthroline, MeCN, 82 °C, sealed tube] as optimal, providing a single reaction product in 80% yield. However, structural elucidation revealed that, in contrast to the carbene insertion reaction of silyldiazoacetate **47** (*vide supra*), nitrene insertion of **60** had occurred at C2 to provide oxazolidinone **63**. Interestingly, we found that the same reaction conducted in CH_2Cl_2, instead of MeCN, provided a completely different product. Extensive 2D NMR analysis revealed this new product to be diacetoxy ketone **64**, whose formation is the result of both C2 oxidation and C10-C14 bond cleavage. Our preliminary mechanistic hypothesis for the formation of **64** is that oxazolidinone **63** is initially generated and that, under the slightly more acidic conditions (CH_2Cl_2 vs. MeCN), C2-aminal exchange takes place followed by a second oxidation that results in the C10-C14 bond cleavage.[37] Evidence to support the potential intermediacy of **63** was gained by converting it to **64** upon submission to the same reaction conditions.

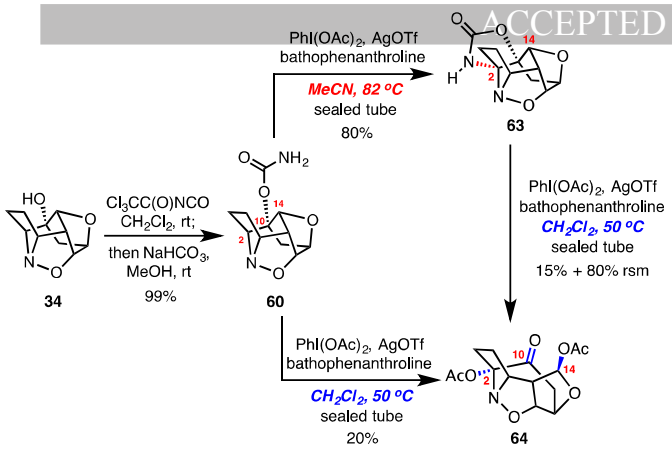

Scheme 15. Oxidative transformations of carbamate **60**.

Given the undesired regioselectivity observed in the oxidative functionalization of carbamate **60**, we wondered whether we could electronically deactivate C2 and direct oxidation to another site on the polycyclic core. Sanford and White have independently demonstrated that C-H bonds proximal to basic amines can be electronically deactivated through protonation or Lewis acid coordination.[38] Unfortunately, this strategy did not translate successfully to our own system. Specifically, submitting either the protonated or BF_3-coordinated adduct **65** to oxidative nitrene insertion conditions led only to decomposition of material (Scheme 16).

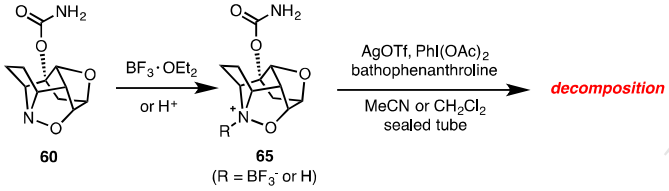

Scheme 16. Attempted nitrene C-H insertion of adduct **65**.

3.7 Sequential C10-C14 oxidative cleavage/reductive pinacol coupling strategy.

While the Ag-mediated oxidative transformations of carbamate **60** failed to deliver the desired C-H insertion product **61**, the formation of diacetoxy ketone **64** was intriguing. Although not part of the initial strategy, the C14 position was modified during the bond cleavage event to the aldehyde oxidation state. This led us to consider whether it would be possible to achieve this same bond cleavage while avoiding C2 oxidation to produce ketone **66** (Scheme 17). Further, **66** might be oxidized to lactone **67** and a subsequent lactone-ketone pinacol coupling could re-unite C10 and C14 to produce the dihydroxylated virosaine core **68**.

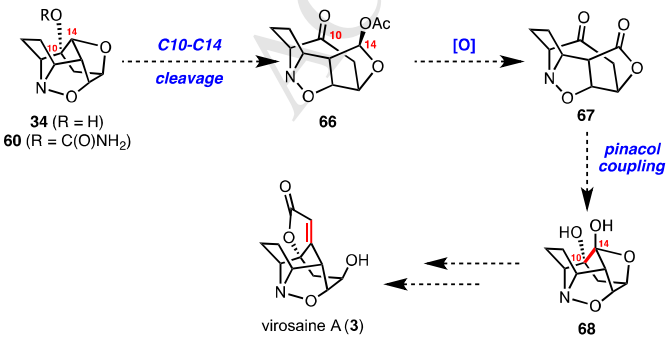

Scheme 17. Sequential C10-C14 oxidative cleavage/reductive pinacol coupling strategy to functionalize C14.

A series of oxidants were screened with both alcohol **34** and carbamate **60** but all failed to induce selective cleavage of the C10-C14 bond (Scheme 18). In contrast, we found that treating alcohol **34** with He's nitrene insertion conditions, as above, resulted in complementary selectivity to that observed for carbamate **60**. Specifically, the reaction produced tetracycles **69** and **70**, each resulting from exclusive C2-C10 bond cleavage followed by further oxidation to the N-alkoxylactam.[39] As with the nitrene chemistry above, attempts to deactivate C2 *via* protonation or BF_3-coordination of the isoxazolidine nitrogen failed to alter the course of the reaction.[38]

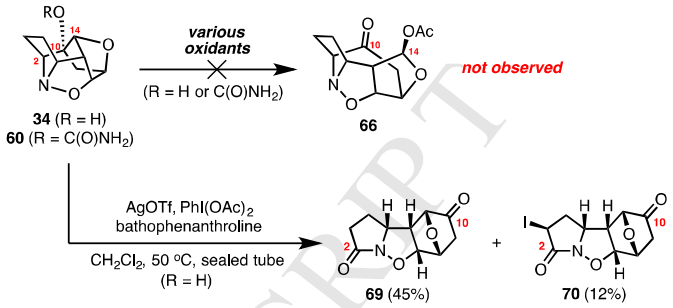

Scheme 18. Oxidative C2-C10 bond cleavage of alcohol **34**.

3.8 Directed lithiation approach to functionalize C14 of the virosaine core.

The lack of reactivity at C14 suggested that a combination of unfavourable steric and stereoelectronic properties were at play. Indeed, Lee has elegantly demonstrated that bridgehead positions vicinal to an oxygen atom are inductively deactivated towards C-H insertion. Geometrical constraints prevent efficient n(O) → σ*(C-H) electron delocalization and thus the main influence is the electronegativity of the oxygen.[26e] Further assessment of the potential sites of reactivity using both NMR and computational analysis on alcohol **34** provided additional insight into this lack of reactivity (Figure 3).[26c,26g,40] Specifically, NMR analysis revealed that both H14 and C14 were the most downfield signals in their respective NMR spectra, suggesting that this position was in fact more electron deficient than we had initially anticipated. Consistent with this notion, the NPA partial charge of C14 was calculated to be significantly more positive than both C2 or C9 and the C14-H14 bond was calculated to have the lowest energy HOMO of all C-H bonds in **34**. These observations were consistent with the observed selectivity for carbene and nitrene insertion at C9 and C2 over the desired position at C14.[41]

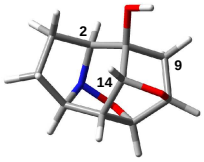

34: "top-down" perspective

Site	^{1}H (δ, ppm)	^{13}C (δ, ppm)	NPA partial atomic charge on carbon	C-H HOMO Energy (eV)
2	3.59	66.8	-0.037	-13.69
9	1.73	45.5	-0.423	-13.71
14	4.72	85.7	+0.095	-14.48

Figure 3. Evaluation of the potential sites of reactivity in **34** by NMR chemical shift assessment and natural population analysis (NPA)/natural bond orbital (NBO) analysis of the energy-minimized structure determined at the B3LYP/6-311++G** level of theory.

The apparent electron-deficient nature of C14 suggested an alternative approach to C-H functionalization. Specifically, we postulated that it might be possible to carry out a selective directed deprotonation at C14 to produce a metalated intermediate that could be functionalized through the addition of a suitable electrophile.[42] We thus examined both tertiary and secondary carbamates **71** and **72**, easily prepared from **34** *via* acylation with $ClC(O)NEt_2$ or sequential addition of carbonyl diimidazole and *n*-butylamine, respectively (Scheme 19). All attempts at directed lithiation with tertiary carbamate **71** returned only starting material. Gratifyingly, in contrast, we found that **72**

could be lithiated selectively at C14 upon treatment with 2.2 equiv. of *s*-BuLi, as judged by quenching of the organolithium intermediate **73** with benzaldehyde to form alcohol **74** in 43% yield. The stronger directing group ability of a metalated secondary carbamate has been noted in other studies.[43,44] With a method in place for selective C14 functionalization, we attempted to trap lithiated intermediate **73** with ethyl bromoacetate. However, instead of generating the desired product **75**, brominated carbamate **76** was obtained in low yield resulting from lithium-bromide exchange. Attempts at transmetalation using CuCN, Li(2-thiophenyl)CuCN or $MgBr_2$ failed to promote direct alkylation with ethyl iodooacetate. In addition, several other carbon-based electrophiles also failed to produce the desired products.[45] While direct installation of the acetate unit could not be accomplished, the bromide **76** was a potential candidate for elaboration. Optimization revealed that **76** could be obtained in 70% yield simply by quenching the dilithiated intermediate **73** with Br_2.

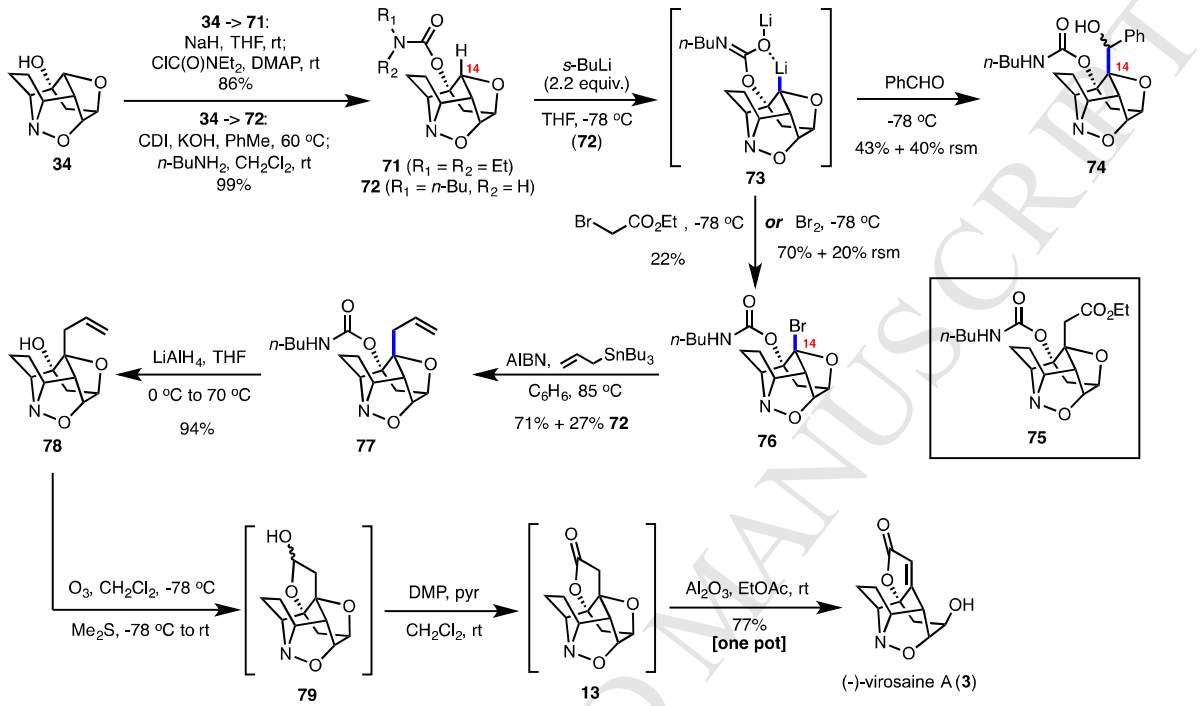

Scheme 19. Synthesis of (-)-virosaine A (**3**).

With a bromide handle in place at C14, subsequent Keck allylation delivered allylated carbamate **77** in 71% yield.[46] Under these conditions, a modest amount of debrominated carbamate **72** was also generated (27% yield) but could be conveniently recycled through the sequence. Carbamate removal was then smoothly carried out *via* reduction using $LiAlH_4$ to deliver alcohol **78** in 94% yield. In order to construct the final ring of the natural product, we subjected **78** to ozone followed by workup with dimethylsulfide and obtained lactol **79**. The crude reaction mixture also contained a minor amount of lactone **13**. As a result, we submitted the mixture directly to Dess-Martin oxidation to exclusively provide lactone **13**. Serendipitously, when we attempted to purify **13** by silica gel flash chromatography, we observed the formation of virosaine A (**3**). However, subsequent attempts to replicate this silica gel-mediated rearrangement (**13→3**) provided inconsistent results that led us to screen other conditions for the transformation. Gratifyingly, we found that simply submitting **13** to activated neutral alumina effected a smooth and reproducible rearrangement to provide **3**. This sequence of ozonolysis, DMP oxidation and fragmentation could be efficiently carried out in a single pot and afforded virosaine A (**3**) directly from alcohol **78** in an excellent 77% yield.

4. Conclusions

In summary, we have developed a concise enantioselective route to access virosaine A (**3**) that proceeds in 10 steps and 9% overall yield. Our synthetic strategy was built around a bio-inspired cascade reaction sequence that allowed rapid construction of the caged polycyclic core of the natural product. Furthermore, after identifying a synthetic limitation of the furan/2-bromoacrolein Diels-Alder reaction, we were required to investigate several methods for late-stage C-H functionalization to completely furnish the carbon framework of **3**. Ultimately, these C-H functionalization studies provided valuable information on the differences in reactivity between several positions on the virosaine core and reinforced the importance that method selection holds when applying a late-stage C-H functionalization strategy on a complex molecule. Finally, a combination of NMR and computational analyses provided a foundation for the successful implementation of a directed lithiation/bromination sequence to selectively functionalize C14 and complete the synthesis of **3**.

5. Experimental

Detailed experimental procedures and characterization data are provided in the Supporting Information associated with this article.

Acknowledgements

This work was supported by the Natural Science and Engineering Research Council of Canada (NSERC). J.M.E.H. thanks NSERC and the Walter C. Sumner Foundation for postgraduate fellowships. We thank Prof. Tristan Lambert (Columbia University) for helpful discussions.

References

[1] For general reviews on the *Securinega* alkaloids, see: (a) Wehlauch R, Gademann K. *Asian J. Org. Chem.* 2017; doi: 10.1002/ajoc.201700142; (b) Chirkin, E.; Atkatlian, W.; Porée, F.-H. In *The Alkaloids*; Knölker, H.-J., Ed.; Academic Press: New York, 2015; Vol. 74, pp 1-120; (c) Zhang W, Li J-Y, Lan P, Sun P-H, Wang Y, Ye W-C, Chen W-M. *J. Chin. Pharm. Sci.* 2011; 20:203; (d) Snieckus, V. In *The Alkaloids*; Manske, R. H. F., Ed.; Academic Press: New York, 1973; Vol. 14, pp 425-503.

[2] For reviews on the synthesis of *Securinega* alkaloids, see Ref. 1 and Weinreb, SM. *Nat. Prod. Rep.* 2009; 26:758.

[3] (a) Horii Z, Hanaoka M, Yamawaki Y, Tamua T, Saito S, Shigematsu N, Kotera K, Yoshikawa H, Sato Y, Nakai H, Sugimoto N, *Tetrahdron*. 1967; 23:1165; (b) Honda T, Namiki H, Kudoh M, Watanabe N, Nagase H, Mizutani H. *Tetrahedron Lett.* 2000; 41:5927; (c) Liras S, Davoren JE, Bordner J. *Org. Lett.* 2001; 3:703; (d) Alibés R, Ballbé M, Busqué F, de March P, Elias L, Figueredo M, Font J. *Org. Lett.* 2004; 6:1813; (e) Honda T, Namiki H, Kaneda K, Mizutani H. *Org. Lett.* 2004; 6:87; (f) Dhudshia B, Cooper BFT, Macdonald CLB, Thadani AN. *Chem. Commun.* 2009; 463; (g) González-Gálvez D, García-García E, Alibés R, Bayón P, de March P, Figueredo M, Font J. *J. Org. Chem.* 2009; 74:6199; (h) Chen J-H, Levine SR, Buergler JF, McMahon TC, Medeiros MR, Wood JL. *Org. Lett.* 2012; 14:4531; (i) Zheng X, Liu J, Ye C-X, Wang A, Wang A-E, Huang P-Q. *J. Org. Chem.* 2015; 80:1034.

[4] Zhao B-X, Wang Y, Zhang D-M, Huang X-J, Bai L-L, Yan Y, Chen J-M, Lu T-B, Wang Y-T, Zhang Q-W, Ye W-C. *Org. Lett.* 2012; 14:3096.

[5] For a review on the occurrence and biosynthetic origins of enantiomeric natural products, see: Finefield JM, Sherman DH, Kreitman M, Williams RM. *Angew. Chem. Int. Ed.* 2012; 51:4802.

[6] For the occurrence of the isoxazolidine moiety in natural products, see: (a) Berthet M, Cheviet T, Dujardin G, Parrot I, Martinez J. *Chem. Rev.* 2016; 116:15235, and references therein; (b) Nge C-E, Sim K-S, Lim S-H, Thomas NF, Low Y-Y, Kam T-S. *J. Nat. Prod.* 2016; 79:2709.

[7] Zhao B-X, Wang Y, Zhang D-M, Jiang R-W, Wang G-C, Shi J-M, Huang X-J, Chen W-M, Che C-T, Ye W-C. *Org. Lett.* 2011; 13:3888.

[8] Parry RJ. *Bioorg. Chem.* 1978; 7:277.

[9] (a) Miyatake-Ondozabal H, Bannwart LM, Gademann K. *Chem. Commun.* 2013; 125:648; (b) Wei H, Qiao C, Liu G, Yang Z, Li C-C. *Angew. Chem. Int. Ed.* 2013; 52:620.

[10] Intramolecular cycloaddition of **12** would proceed with the nitrone adding across the alkene with the opposite regiochemistry as compared to **9** or **10**.

[11] For recent total syntheses employing biomimetic [3+2] nitrone cycloadditions, see Ref 10 and: (a) Ma N, Yao Y, Zhao B-X, Wang Y, Ye W-C, Jiang S. *Chem. Commun.* 2014; 50:9284; (b) Hong AY, Vanderwal CD. *J. Am. Chem. Soc.* 2015; 137:7306; (c) Hong AY, Vanderwal CD. *Tetrahedron*. 2016; 73:4160.

[12] For synthetic studies towards pyridomacrolidin employing a biomimetic [3+2] nitrone cycloaddition, see: (a) Irlapati NR, Baldwin JE, Adlington RM, Pritchard GJ. *Org. Lett.* 2003; 5:2351; (b) Irlapati NR, Baldwin JE, Adlington RM, Pritchard GJ, Cowley AR. *Tetrahedron.* 2006; 62:4603.

[13] For computational studies of biosynthetic [3+2] nitrone cycloadditions, see: (a) Krenske EH, Patel A, Houk KN. *J. Am. Chem. Soc.* 2013; 135:17638; (b) Painter PP, Pemberton RP, Wong BM, Ho KC, Tantillo DJ. *J. Org. Chem.* 2014; 79:432.

[14] For an initial communication on this synthesis of virosaine A, see: Hughes JME, Gleason JL. *Angew. Chem. Int. Ed.* 2017; 56:10830..

[15] For a review on furan Diels-Alder reactions, see: Kappe CO, Murphree SS, Padwa A. *Tetrahedron*. 1997; 53:14179.

[16] For select examples of nitrone formation/[3+2] cycloaddition cascade reactions in total synthesis, see: (a) Davison EC, Fox ME, Holmes AB, Roughley SD, Smith CJ, Williams GM, Davies JE, Raithby PR, Adams JP, Forbes IT, Press NJ, Thompson MJ. *J. Chem. Soc., Perkin Trans. 1.* 2002; 1494; (b) Stockman RA, Sinclair A, Arini LG, Szeto P, Hughes DL. *J. Org. Chem.* 2004; 69:1598; (c) Karatholuvhu MS, Sinclair A, Newton AF, Alcaraz M-L, Stockman RA, Fuchs PL. *J. Am. Chem. Soc.* 2006; 128:12656; (d) Wilson MS, Padwa A. *J. Org. Chem.* 2008; 73:9601; (e) Burrell AJM, Coldham I, Oram N. *Org. Lett.* 2009; 11:1515; (f) Flick AC, Caballero MJA, Padwa A. *Tetrahedron*. 2010; 66:3643.

[17] Grigg R, Markandu J. *Tetrahedron Lett.* 1989; 30:5489.

[18] (a) Brown HC, Brown CA. *J. Am. Chem. Soc.* 1963; 85:1005; (b) Brown CA, Ahuja VK. *J. Org. Chem.* 1973; 38:2226; (c) Brown CA, Ahuja VK. *J. Chem. Soc., Chem. Commun.* 1973; 553.

[19] For a review on the synthetic utility of nickel boride, see: Khurana JM, Gogia A, *Org. Prep. Proc. Int.* 1997; 29:1.

[20] Lindlar reduction conditions were found to be less consistant and were plagued by significant amounts of an over-oxidation byproduct (see Supporting Information).

[21] Casey ML, Kemp DS, Paul KG, Cox DD. *J. Org. Chem.* 1973; 38:2294.

[22] Schindler CS, Carreira EM. *Chem. Soc. Rev.* 2009; 38:3222.

[23] Corey EJ, Loh TP. *Tetrahedron Lett.* 1993; 34:3979.

[24] Several other oxazaborolidine catalysts led to similar results: (a) Corey EJ, Shibata T, Lee TW. *J. Am. Chem. Soc.* 2002; 124:3808; (b) Ryu DH, Corey EJ. *J. Am. Chem. Soc.* 2003; 125:6388; (c) Liu D, Canales E, Corey EJ. *J. Am. Chem. Soc.* 2007; 129:1498.

[25] For select reviews on C-H functionalization, see: (a) Godulal K, Sames D. *Science*. 2006; 312:67; (b) Davies HML, Manning JR. *Nature.* 2008; 451:417; (c) Gutekunst WR, Baran PS. *Chem. Soc. Rev.* 2011; 40:1976; (d) McMurray L, O'Hara F, Gaunt MJ. *Chem. Soc. Rev.* 2011; 40:1885; (e) Yamaguchi J, Yamaguchi AD, Itami K. *Angew. Chem. Int. Ed.* 2012; 51:8960; (f) Chen DY-K, Youn SW. *Chem. Eur. J.* 2012; 18:9452; (g) Egger J, Carreira EM. *Nat. Prod. Rep.* 2014; 31:449; (h) Qiu Y, Gao S. *Nat. Prod. Rep.* 2016; 33:562; (i) Davies HML, Morton D. *J. Org. Chem.* 2016; 81:343.

[26] For recent total syntheses involving late-stage C(sp^3)-H functionalizations, see: (a) Hinman A, Du Bois J. *J. Am. Chem. Soc.* 2003; 125:11510; (b) Bisai A, West SP, Sarpong R. *J. Am. Chem. Soc.* 2008; 130:7222; (c) Chen K, Baran PS. *Nature*. 2009; 459:824; (d) Stang EM, White MC. *Nat. Chem.* 2009; 1:547; (e) Yun SY, Zheng J-C, Lee D. *J. Am. Chem. Soc.* 2009; 131:8413; (f) Huters AD, Quasdorf KW, Styduhar ED, Garg NK. *J. Am. Chem. Soc.* 2011; 133:15797; (g) Kawamura S, Chu H, Felding J, Baran PS. *Nature*. 2016; 532:90; (h) McCallum ME, Rasik CM, Wood JL, Brown MK. *J. Am. Chem. Soc.* 2016; 138:16616; (i) Hung K, Condakes ML, Morikawa T, Maimone TJ. *J. Am. Chem. Soc.* 2016; 138:16616; (j) Liu C, Chen R, Shen Y, Liang Z, Hua Y, Zhang Y. *Angew. Chem. Int. Ed.* 2017; 56:8187.

[27] (a) Schindler CS, Stephenson CRJ, Carreira EM. *Angew. Chem. Int. Ed.* 2008; 47:8852; (b) Diethelm S, Schindler CS, Carreira EM. *Org. Lett.* 2010; 12:3950; (c) Zipfel HF, Carreira EM. *Org. Lett.* 2014; 16:2854.

[28] See the Supporting Information for a summary of the nucleophiles screened.

[29] The significant loss in mass balance during this reaction was attributed to decomposition of material under the reaction conditions.

[30] For select reviews on carbene C-H insertion, see: (a) Davies HML, Beckwith REJ. *Chem. Rev.* 2003; 103:2861; (b) Doyle MP, Duffy R, Ratnikov M, Zhou L. *Chem. Rev.* 2010; 110:704; (c) Doyle MP, Ratnikov M, Liu Y. *Org. Biomol. Chem.* 2011; 9:4007; (d) Lombard FJ, Coster MJ. *Org. Biomol. Chem.* 2015; 13:6419; (e) Ford A, Miel H, Ring A, Slattery CN, Maquire AR, McKervey MA. *Chem. Rev.* 2015; 115:9981.

[31] (a) Osawa E, Tahara Y, Togashi A, Iizuka T, Tanaka N, Kan T. *J. Org. Chem.* 1982; 47:1923; (b) Sonawane HR, Bellur NS, Ahuja JR, Kulkarni DG. *J. Org. Chem.* 1991; 56:1434; (c) Grainger RS, Owoare RB. *Org. Lett.* 2004; 6:2961; (d) Kawasumi M, Kanoh N, Iwabuchi Y. *Org. Lett.* 2011; 13:3620; (e) Jansone-Popova S, May JA. *Tetrahedron*. 2016; 72:3734.

[32] Maas, G. In *The Chemistry of Organic Silicon Compounds*; Rappoport, Z., Apeloig, Y., Eds.; Wiley, Chichester, 1998; Vol. 2, pp 703-778.

[33] We also briefly investigated the use of donor/acceptor carbenoids for the C-H insertion reaction but were unsuccessful in achieving the desired transformation.

[34] For related carbene N-O insertions, see: (a) Manning JR, Davies HML. *Tetrahedron.* 2008; 64:6901; (b) Xu X, Ratnikov MO, Zavalij PY, Doyle MP. *Org. Lett.* 2011; 13:6122.

[35] For select reviews on nitrene C-H insertions, see: (a) Li Z, He C. *Eur. J. Org. Chem.* 2006; 4313; (b) Zalatan DN, Du Bois J. *Top. Curr. Chem.* 2010; 292:347; (c) Collet F, Lecot C, Dauben P. *Chem. Soc. Rev.* 2011; 40:1926; (d) Roizen JL, Harvey ME, Du Bois J. *Acc. Chem. Res.* 2012; 335:807.

[36] For select examples of intramolecular nitrene C-H insertions in total synthesis, see Ref. **26a, 26f** and: (a) Ciufolini MA, Byrne NE. *J. Am. Chem. Soc.* 1991; 113:8016; (b) Wehn PM, Du Bois J. *J. Am. Chem. Soc.* 2002; 124:12950; (c) Fleming JJ, Du Bois J. *J. Am. Chem. Soc.* 2006; 128: 3926; (d) Tanino T, Ichikawa S, Shiro M, Matsuda A. *J. Org. Chem.* 2010; 75:1366; (e) Quasdorf KW, Huters AD, Lodewyk MW, Tantillo DJ, Garg NK. *J. Am. Chem. Soc.* 2012; 134:1396; (f) Styduhar ED, Huters AD, Weires NA, Garg NK. *Angew. Chem. Int. Ed.* 2013; 52:12422; (g) Weires NA, Styduhar ED, Baker EL, Garg NK. *J. Am. Chem. Soc.* 2014; 136:14710.

[37] Alternatively, C10-C14 bond cleavage may occur through direct activation of **63** with PIDA followed by aminal exchange.

[38] (a) Lee M, Sanford MS. *J. Am. Chem. Soc.* 2015; 137:12796; (b) Howell JM, Feng K, Clark JR, Trzepkowski LJ, White MC. *J. Am. Chem. Soc.* 2015; 137:14590.

[39] For an example of a similar oxidative C-C bond fragmentation, see: Hamlin AM, Lapointe D, Owens K, Sarpong R. *J. Org. Chem.* 2014; 79:6783.

[40] (a) Michaudel Q, Journot G, Regueiro-Ren A, Goswami A, Guo Z, Tully TP, Zou L, Ramabhadran RO, Houk KN, Baran PS. *Angew. Chem. Int. Ed.* 2014; 53:12091; (b) Chen MS, White MC. *Science*. 2007; 318:783; (c) Bigi MA, Liu P, Zou L, Houk KN, White MC. *Synlett.* 2012; 23:2768; (d) Gormisky PE, White MC. *J. Am. Chem. Soc.* 2013; 135:14052.

[41] See the Supporting Information for details.

[42] For selected examples of directed lithiation at sp^3 centers in total synthesis, see **Ref. 26b** and: (a) Wilkinson TJ, Stehle NW, Beak P. *Org. Lett.* 2000; 2:155; (b) Johnson TA, Curtis MD, Beak P. *J. Am. Chem. Soc.* 2001; 123:1004; (c) Vu VH, Louafi F, Girard N, Marion R, Roisnel T, Dorcet V, Hurvois J-P. J. *Org. Chem.* 2014; 79:3358; (d) Varela A, Garve LKB, Leonori D, Aggarwal VK, *Angew. Chem. Int. Ed.* 2017; 56:2127.

[43] Beak P, Meyers AI. *Acc. Chem. Res.* 1986; 19:356.

[44] For a review on the complex-induced proximity effect, see: Whisler MC, MacNeil S, Snieckus V, Beak P. *Angew. Chem. Int. Ed.* 2004; 43:2206.

[45] See Supporting Information for a summary of electrophiles screened.

[46] Keck GE, Yates JB. *J. Am. Chem. Soc.* 1982; 104:5829.